Improvement of PMSM loss estimation accuracy focusing on over 50,000rpm

Atsuya Sano [1)] **Kan Akatsu** [1)]

1) Yokohama National University, Yokohama, Japan

E-mail: akatsu-kan-py@ynu.ac.jp

ABSTRACT: Permanent Magnet Synchronous Motor (PMSM) offers high efficiency and high-power density, however it also presents resource-related risks due to the use of rare-earth magnets and copper. As a solution, ultra-high-speed, miniaturized PMSM aimed at conserving resources is attracting attention. However, there are no studies that evaluate losses in the ultra-high-speed operating region using actual machine measurements and analysis. In this paper, we target a PMSM equivalent to 8-poles with a maximum speed of 50,000 rpm to measure actual machine losses and assess the accuracy of iron loss estimation. We clarify the differences between the actual machine measurements and the analysis results at a maximum electrical angular frequency of 3.3 kHz.

KEY WORDS: High speed motor, Iron loss, IPMSM

1. INTRODUCTION

PMSM has high-efficiency and high-power density and it is used in various industrial equipment such as automobiles, rolling stock, and so on. However, PMSM presents resource-related risks due to the use of rare-earth magnets and copper, both of which are expected to become depleted. Therefore, compact, ultra-high-speed PMSM is attracting attention for the purpose of resource conservation. One issue, however, is the increase in losses and the accompanying temperature rise during ultra- high-speed operation. Therefore, accurate loss estimation at ultra-high speeds is needed to establish an efficient cooling method and to develop a highly efficient ultra-high-speed motor.

Iron loss is a major source of losses in PMSM and is particularly dominant at high speeds. Therefore, various iron loss models have been developed to accurately predict iron loss. The binomial model is commonly used for general iron loss estimation due to its simplicity, while the ternary model, which separates abnormal eddy current losses, is also widely used [(1)~(6)]. Additionally, iron loss is influenced by various physical factors, such as temperature, compressive stress, DC bias, and PWM harmonics. Iron loss models that account for these factors have been developed and evaluated in (7)(8)(9). However, there has not been evaluated iron loss using an actual PMSM with an electrical angular frequency of 3.3 kHz. This paper, therefore, evaluates the iron loss at a maximum electrical angular frequency of 3.3 kHz using an actual PMSM.

2. EQUIPMENT UNDER TEST MOTOR

2.1 Equipment Under Test Motor Characteristics

In this study, it is necessary to design equipment under test (EUT) motor to be driven at a maximum electric angular frequency of 3.3 kHz. The maximum measurable speed is determined to be 20,000 rpm due to the test environment limitation, including the brake and torque meter used during the actual machine test. Therefore, the number of poles of the EUT motor is set to 20. Fig. 1 shows the designed EUT motor model. The structural feature of the EUT motor is grooves in the rotor and stator [(10)]. As shown in Fig. 2, these grooves reduce cogging torque by 77% ang torque ripple at 20,000rpm by 64%. Tab. 1 shows the EUT motor specifications. In this EUT motor, wire electrical discharge machining (EDM) is used to eliminate the effect of residual strain generated in the core punching process on iron loss characteristics. Stranded wire is used to prevent increased copper loss due to skin effect at ultra-high-speed rotation.

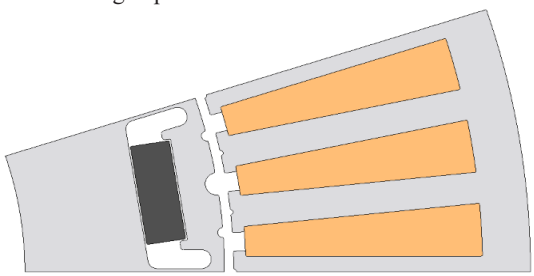

Fig. 1: EUT motor model

Tab. 1: EUT motor specifications

Parameters	Value
Number of poles / slots	20 / 60
Stator / Rotor O.D. [mm]	136 / 90
Stack length [mm]	70
Core thickness [mm]	0.2
Core machining	Wire EDM
Magnet	Nd – Fe – B
Number of magnet [/pole]	8
Winding	Stranded wire
Number of turns [turn/slot]	8 (8 parallel)
Winding method	Distributed winding
Motor output [kw]	5
Maximum speed [rpm]	20,000
Maximum torque [Nm]	10
Inverter voltage [VDC]	230
Maximum current [Apeak]	31

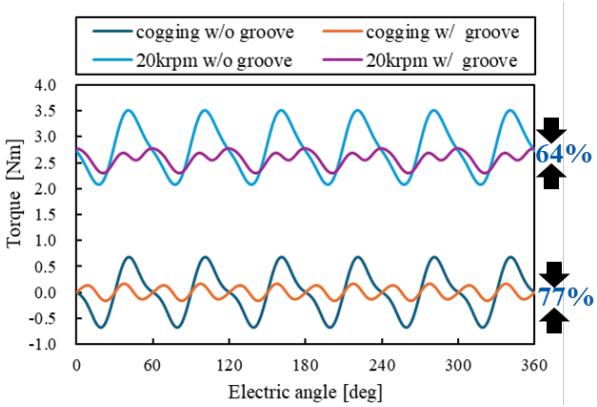

Fig. 2: Comparison of torque waveforms with and without grooves

2.2 Magnet Strength and Core Stacking factor Adjustment Between Actual Motor and Analytical Model

The magnet strength of the actual machine and the analytical model differ due to the manufacturing process. Therefore, the measured magnetic flux density on the rotor surface is used to adjust the analytical model by modifying the magnet characteristics. Fig. 3 and Fig. 4 show the experimental environment and results. In Fig. 4 the fundamental component is adjusted by setting the B_r of the magnet such as the residual flux density to 87.86% of the catalog value in the analysis. Since the stacking factor also effects to the back-emf waveform, we counted the number of stacking electrical steel sheet. The result was 96.3% of the core stacking length; 70mm. Fig. 5 shows the back-emf waveform comparison between the experimental result and simulation result under the ambient temperature condition. They are well confirmed. However, the permanent magnet strength varies with the temperature, we estimate the magnet temperature so that the measured back-emf matches simulated back-emf.

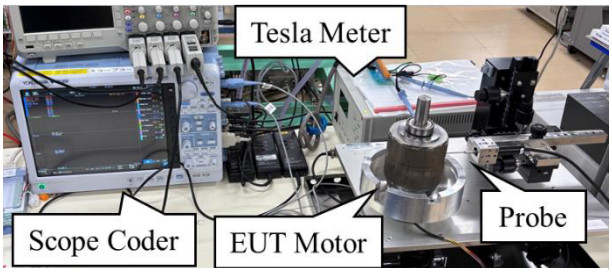

Fig. 3: Magnet flux density measurement equipment

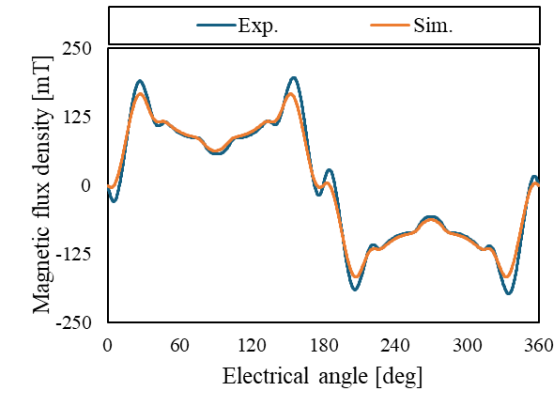

(a)

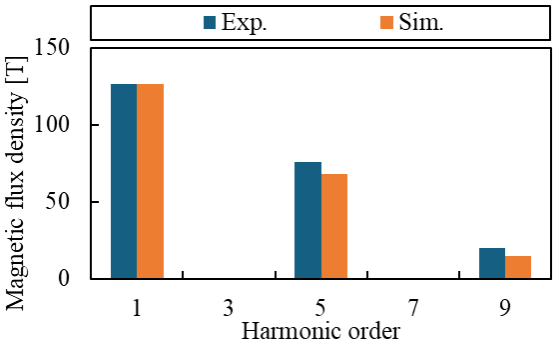

(b)

Fig. 4: Magnetic flux density of rotor surface (a)waveforms, (b)FFT

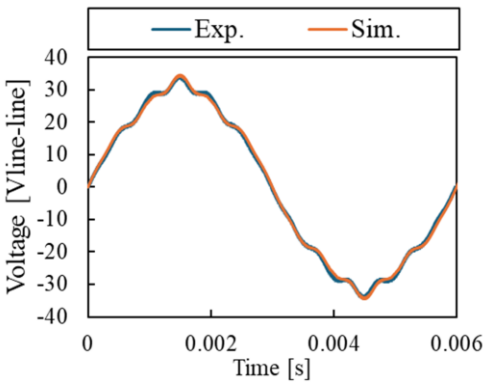

Fig. 5 Back-EMF waveforms of experimental result and simulation result

3. NO –LOAD LOSS MEASUREMENT AND IRON LOSS EVALUATION

In this study, rotors with and without magnets are used to separate iron loss from the measured loss including mechanical loss. Since the iron loss and mechanical loss can be measured for the rotor with magnet and the mechanical loss for the rotor without magnet, the iron loss is separated by taking the difference. Fig. 6 shows the measurement environment. The EUT motor is rotated by the load motor, and the speed and torque are measured with a scope coder to calculate the loss. A thermocouple is attached to the surface of the stator core to obtain the temperature at the same time.

3.1 Confirmation of temperature dependence and effect of circulating current

To confirm the temperature dependence of iron loss and mechanical loss, we measured the transition between torque and temperature at a constant rotational speed. Fig. 7 shows the measurement results for a rotor with and without magnet. From Fig. 7, it is obvious that temperature effects to the losses not only the rotor with magnets but also the rotor without magnets, the careful temperature control is needed. Actually, we do not have a temperature sensor with the magnet, we measured and controlled stator temperature, and we estimate the magnet temperature.

The coils of the EUT motor are stranded wires, and there is concern that circulating current may flow due to variations in the path of each wire. To confirm the effect of the circulating current on the measurement results, measurements are conducted with the terminal tips of each phase shorted and open. Fig. 8 shows terminal condition when it is opened. Tab. 2 shows the experimental conditions and Fig. 9 shows the measurement results. From Fig. 9, there is no effect of the circulating current, and the difference in the measurement results can be attributed to the fact that the temperature is acquired from the surface of the stator core.

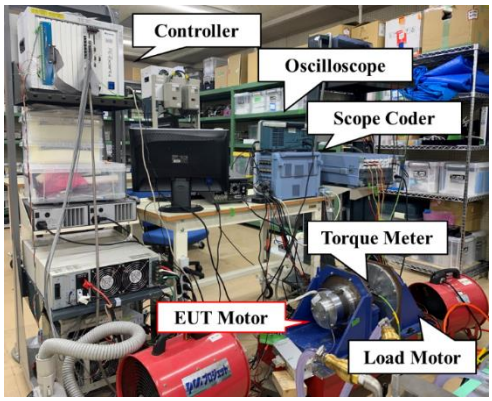

Fig. 6: Experimental environment

Tab. 2: Experiment and Analysis conditions

Parameters	Value
Speed [rpm]	1,000 – 20,000 , Δ 1,000
Current [Apeak]	0
Magnet temperature [°C]	Fig. 11

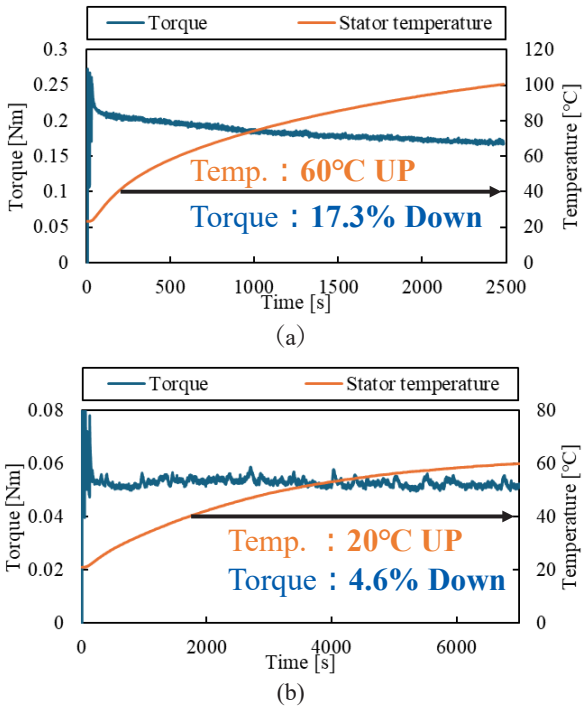

Fig. 7: Time transition of no-load loss
(a) rotor with magnet at 15,000 rpm
(b) rotor without magnet at 20,000 rpm

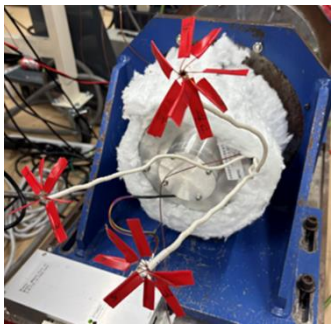

Fig. 8: Terminal open condition

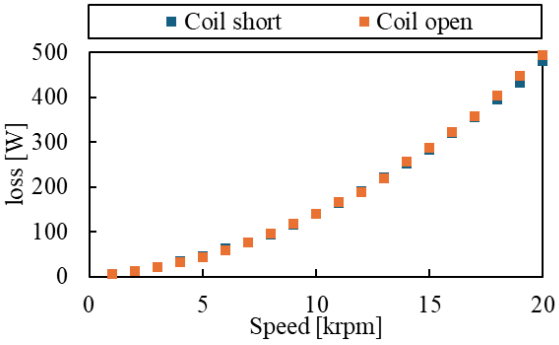

Fig. 9: Effect of circulating current

3.2 Measurement results

Fig. 10 shows the experiment results when the rotor is rotated up to 20,000rpm. Experimental conditions are the same as shown in Tab. 2. In Fig. 10, iron loss is separated from the direction between the results for rotor with magnet and without magnet. Even the rotation speed and its fundamental frequency are very high, the iron loss phenomenon is not strange, it can be estimated from the loss in the lower speed.

3.3 Iron loss estimation

The iron loss model used for iron loss estimation is (1).

$$p = p_h + p_e \quad (1)$$

where p is iron loss density. p_h is hysteresis loss density. p_e is eddy current loss density. Hysteresis loss takes minor loops into account, and eddy current loss is the sum of classical eddy current loss and anomalous eddy current loss.

The iron loss data used for iron loss estimation are measured by laminated bonded ring cores using the same lot of electromagnetic steel plates as the motor, and under the same processing conditions as the motors. However, the maximum frequency is 2 kHz, which is interpolated by the square of the frequency thereafter.

Since iron loss depends on magnetic flux density and magnet temperature affects magnetic flux density, the magnet temperature at the time of loss measurement is estimated. The magnet temperature of the analytical model is changed to match the fundamental component of the back-emf in the analysis with that of the actual motor during loss measurement. Fig. 12 shows the results of magnet temperature estimation.

Fig. 13 shows the comparison between the measured iron loss and estimated iron loss. Fig. 13(a) shows that the estimates are smaller than the experimental values, and Fig. 13(b) shows that the estimation error occurs about 20%.

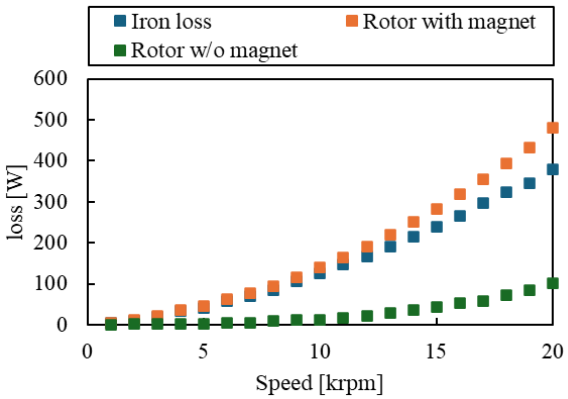

Fig. 10: Measured no-load loss

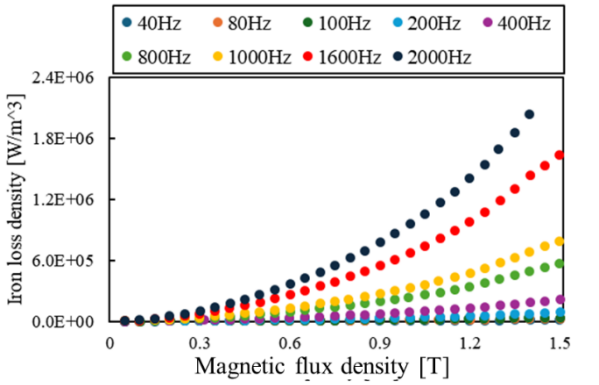

Fig. 11: Iron loss data

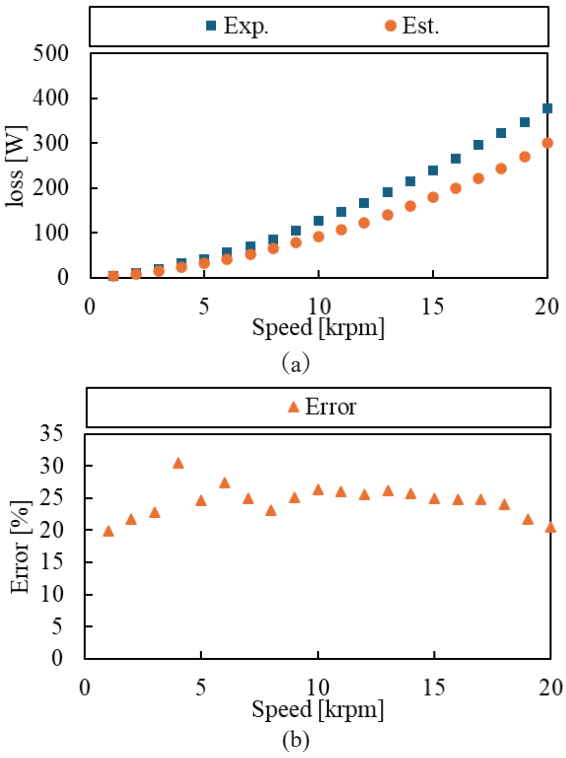

Fig. 12: Iron loss estimation
(a) Iron loss, (b) Estimation error

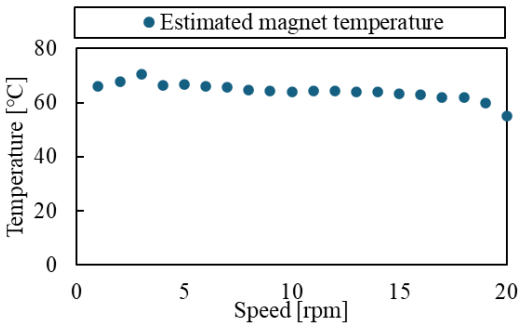

Fig. 13: Estimated magnet temperature under driving.

Tab. 3: Resistance of machined surface

Resistance [Ω]	4.19

Fig. 14: Experimental environment

3.4 Discussion

One probable reason for the iron loss estimation error is the conduction of the machined surface by Wire EDM. Fig. 14 and Tab. 4 shows the experimental environment and measurement results of the resistance value between the top side and the bottom side of the stator core. From Tab. 4, there is continuity on the machined surface. Therefore, it is considered that the experimental value is larger than the estimated value due to the large eddy current flow on the machined surface and the large eddy current loss in the experiment. This will be cleared by the measured iron loss result by using the sample EDM core and eddy current loss analysis results of the stator surface.

4. CONCLUSIONS

In this paper, the iron loss of an ultra-high-speed PMSM is evaluated using an actual motor and an analytical model. Using an analytical model adjusted to the actual motor based on the magnetic flux density on the rotor surface, the iron loss estimation error is about 20%. In the future, we will clarify the influence of the conductivity of the machined surface by Wire EDM on the iron loss estimation error.

Acknowledgment

This paper is based on results obtained from a subcontract from Transmission Research Association for Mobility Innovation (TRAMI) as part of the New Energy and Industrial Technology Development Organization (NEDO) Feasibility Study Program on Energy and New Environmental Technology / Resource saving of electric drive system for automobiles by ultra- high rotation of e-motor. (JPNP14004).

References

(1) D. Kowal, P. Sergeant, L. Dupré and L. Vandenbossche, "Comparison of Iron Loss Models for Electrical Machines With Different Frequency Domain and Time Domain Methods for Excess Loss Prediction," in IEEE Transactions on Magnetics, vol. 51, no. 1, pp. 1-10, Jan. 2015

(2) J. Li, Q. Yang, Y. Li, C. Zhang, B. Qu and L. Cao, "Anomalous Loss Modeling and Validation of Magnetic Materials in Electrical Engineering," in IEEE Transactions on Applied Superconductivity, vol. 26, no. 4, pp. 1-5, June 2016

(3) L. Liu, W. N. Fu, S. Yang and S. L. Ho, "Iron Loss Separation in High Frequency Using Numerical Techniques," in IEEE Transactions on Magnetics, vol. 52, no. 3, pp. 1-4, March 2016

(4) W. Roshen, "Iron Loss Model for Permanent-Magnet Synchronous Motors," in IEEE Transactions on Magnetics, vol. 43, no. 8, pp. 3428-3434, Aug. 2007

(5) Y. Gao, Y. Matsuo, K. Muramatsu, "Investigation on Simple Numeric Modeling of Anomalous Eddy Current Loss in Steel Plate Using Modified Conductivity," in IEEE Transactions on Magnetics, vol. 48, no. 2, pp. 635-638, February 2012

(6) W. Guan, D. Zhang, Y. Zhu, Y. Gao and K. Muramatsu, "Numerical Modeling of Iron Loss Considering Laminated Structure and Excess Loss," in IEEE Transactions on Magnetics, vol. 54, no. 11, pp. 1-4, Nov. 2018

(7) Z. -Q. Zhu et al., "Evaluation of Iron Loss Models in Electrical Machines," in IEEE Transactions on Industry Applications, vol. 55, no. 2, pp. 1461-1472, March-April 2019

(8) G. Liu, M. Liu, Y. Zhang, H. Wang and C. Gerada, "High-Speed Permanent Magnet Synchronous Motor Iron Loss Calculation Method Considering Multiphysics Factors," in IEEE Transactions on Industrial Electronics, vol. 67, no. 7, pp. 5360-5368, July 2020

(9) L. Bi, U. Schäfer and Y. Hu, "A New High-Frequency Iron Loss Model Including Additional Iron Losses due to Punching and Burrs' Connection," in IEEE Transactions on Magnetics, vol. 56, no. 10, pp. 1-9, Oct. 2020

(10) G. -H. Kang, Y. -D. Son, G. -T. Kim and J. Hur, "A Novel Cogging Torque Reduction Method for Interior-Type Permanent-Magnet Motor," in IEEE Transactions on Industry Applications, vol. 45, no. 1, pp. 161-167, Jan.-feb. 2009